Journal Pre-proofs

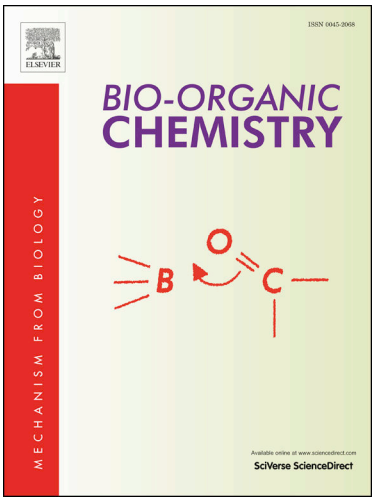

New fused pyrimidine derivatives with anticancer activity: synthesis, topoisomerase II inhibition, apoptotic inducing activity and molecular modeling study

Mohamed T. M. Nemr, Asmaa M. AboulMagd

PII: S0045-2068(20)31431-0
DOI: https://doi.org/10.1016/j.bioorg.2020.104134
Reference: YBIOO 104134

To appear in: *Bioorganic Chemistry*

Received Date: 8 June 2020
Revised Date: 4 July 2020
Accepted Date: 20 July 2020

Please cite this article as: M. T. M. Nemr, A.M. AboulMagd, New fused pyrimidine derivatives with anticancer activity: synthesis, topoisomerase II inhibition, apoptotic inducing activity and molecular modeling study, *Bioorganic Chemistry* (2020), doi: https://doi.org/10.1016/j.bioorg.2020.104134

New fused pyrimidine derivatives with anticancer activity: synthesis, topoisomerase II inhibition, apoptotic inducing activity and molecular modeling study

Mohamed T. M. Nemr [1], Asmaa M. AboulMagd [2*]

[1]Pharmaceutical Organic Chemistry Department, Faculty of Pharmacy, Cairo University, Kasr El-Eini street 11562, Cairo, Egypt.

[2]Pharmaceutical Chemistry Department, Faculty of Pharmacy, Nahda University, Beni-suef, Egypt.

*** Corresponding author email: asmaa.aboulmaged@nub.edu.eg**

Abstract:

A new series of triazolopyrimidines and thiazolopyrimidine hydrobromides was designed and prepared as topoisomerase II inhibitors. Screening of all synthesized compounds was carried out by the National Cancer Institute (NCI) of USA. Activity against 60 human cancer cell lines representing different cancer types was determined. Accordingly, compound **3d** was the most potent inhibitor especially against the renal cell line A498 causing 92.46 % inhibition (IC_{50} = 3.5 μM). Moreover, cell cycle analysis showed cell cycle arrest caused by compound **3d** at the G2/M phase leading to cell proliferation inhibition and pro-apoptotic activity. Also, thiazolopyrimidine **3d** showed potent topoisomerase II inhibitory activity (IC_{50} 2.89 μM) compared to doxorubicin which was used as a reference compound with (IC_{50} 2.67 μM). Moreover, molecular modeling study of the synthesized compounds was performed and revealed the binding interactions of compound **3d** in the binding site of topoisomerase II enzyme rationalizing the significant inhibitory activity of this derivative.

Keywords: triazolopyrimidines, thiazolopyrimidines, topoisomerase II, flow cytometry, apoptosis, molecular docking.

1. Introduction:

Cancer is one of the most common causes of death all over the world. Although advanced techniques for its diagnosis were developed to help in its early detection, there is still an urgent need to discover new efficient antitumor agents on available targets [1]. Renal cancer is one of the most common types of cancer that is responsible for about 1.7% of deaths worldwide according to WHO [2]. On the other hand, topoisomerases I and II (Topo I and II) are considered as attractive agents due to their essential role in DNA replication and transcription [3]. Topoisomerase II inhibitors such as etoposide **I** (ETO), mitoxantrone **II** and doxorubicin **III** are reported as anticancer drugs especially against kidney, breast and lung cancers [4-6] (Fig. 1).

Thiazolopyrimidines are group of heterocyclic compounds of special interest. Several publications mentioned the diverse activity of thiazolo[3,2-a]pyrimidines including antineoplastic, antimicrobial, antioxidant and antiviral [7-13]. Moreover, thiazole derivatives have gained a notable significance due to their use as anticancer agents. Also, pyrimidine moiety constitutes a large number of pharmacologically active compounds especially antineoplastic agents. Since the two heterocyclic rings thiazole and pyrimidine designate two active pharmacophores that are active against cancer, combining the two is anticipated to have a potent effect on their antitumor properties [14-15]. Recently, it was reported that a series of thiazolo[3,2-a]pyrimidine hydrobromides was synthesized and evaluated for their anticancer activity [16-19]. It was found that compound **IV** exhibited significant anticancer activity against liver cancer (hepG-2) cell line (IC_{50} 1.20 μM) [20]. To be more precise, the presence of substituents on the phenyl ring in thiazolo[3,2-a]pyrimidine scaffold contributed to the binding activity of these derivatives to topoisomerase II [12]. Encouraged by the fact that thiazolopyrimidine salts are not a large series and based on the mentioned findings, it was of interest to prepare a series of thiazolo[3,2-a]pyrimidine and 1,2,4-triazolo[4,3-a]pyrimidine (as isosteres of thiazolo[3,2-a]pyrimidine) (**2a-c, 3a-e**) via a facile convenient method and investigate their antineoplastic activity against 60 different cancer cell lines. Additionally, topoisomerase II inhibitory activity evaluation was performed in an attempt to explain their biological activity. Furthermore, docking study was carried out for all the synthesized compound to predict their binding manner with the enzyme compared to doxorubicin as standard topoisomerase II inhibitor.

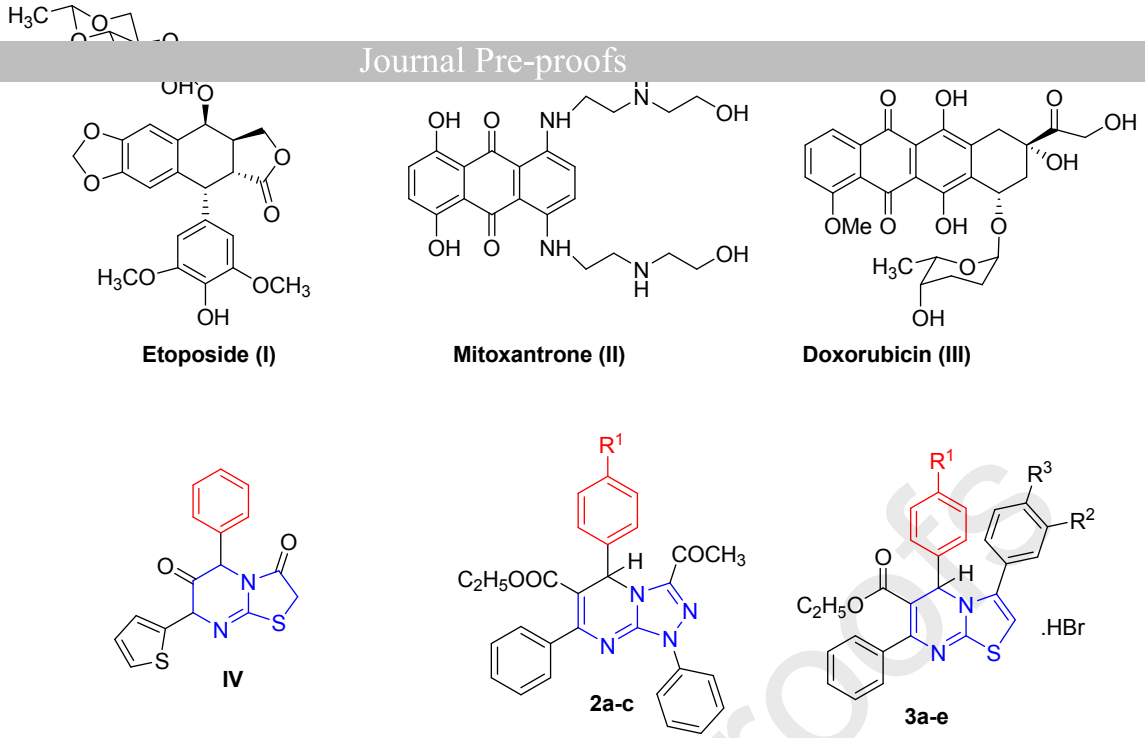

Fig. 1. Reported topoisomerase II inhibitors and scaffold of target compounds

2. Results and discussion:

2. 1. Synthesis

The parent compounds **1a-c** were prepared according to the standard Biginelli conditions on refluxing the substituted aldehydes, thiourea and ethyl benzoyl acetate for 3h in the presence of catalytic amount of concentrated hydrochloric acid to yield tetrahydro- pyrimidine-2-thione derivatives **1a-c** [21]. In the present work, compounds **1a-c** as a good example of 2-thioxopyrimidines react with the reactive hydrazonoyl chloride (**4**) in the presence of a catalytic amount of TEA to afford the corresponding 1,2,4-triazolo[4,3-a]pyrimidine derivatives **2a-c, Scheme 1**. The proposed reaction mechanism involved initial formation of thiohydrazonate (**V**), which will undergo intermolecular cyclization to afford intermediate **VI** which will rearrange to intermediate **VII** that upon losing H_2S afforded the target compound 1,2,4-triazolo[4,3-a]pyrimidine as reported [22]. The structure of the title compounds **2a-c** was confirmed by spectral data. IR spectra of these title compounds revealed the disappearance of NH peaks of **1a-c** at 3300-3150 cm^{-1} which was characteristic to amino group in the starting compounds and the characteristic appearance of additional the carbonyl group at 1701-1680 cm^{-1}. ^{1}H-NMR spectrum of compounds **2a-c** showed in addition to the expected δ values for the ethyl ester group, aromatic hydrogens, and an aliphatic signal at approximately 2.6 ppm due to a new CH_3 group. On the other hand, literature survey revealed that the reaction of tetrahydropyrimidine-2-thiones with phenacyl bromides in either glacial acetic acid [22-23] or ethanol [24] gave the corresponding thiazolo[3,2-a]pyrimidines. In the present

investigation, the pyrimidinethiones **1a-c** were reacted with *m*-nitrophenacyl bromide and *p*-nitrophenacyl bromide to afford the corresponding thiazolopyrimidines hydrobromides **3a-e, Scheme 1**. The latter compounds **3a-e** were confirmed by the disappearance of the NH peaks in IR spectra. ^{1}H-NMR spectra of compound **3a-e** revealed disappearance of the two singlet signals corresponding to two NH of the starting derivative **1a-c** and the appearance of the ethyl ester group in addition to the additional protons in aromatic region due to presence of additional phenyl ring added from substituted phenacyl bromide moiety which also appears as additional signals in their ^{13}C-NMR spectra.

Scheme 1

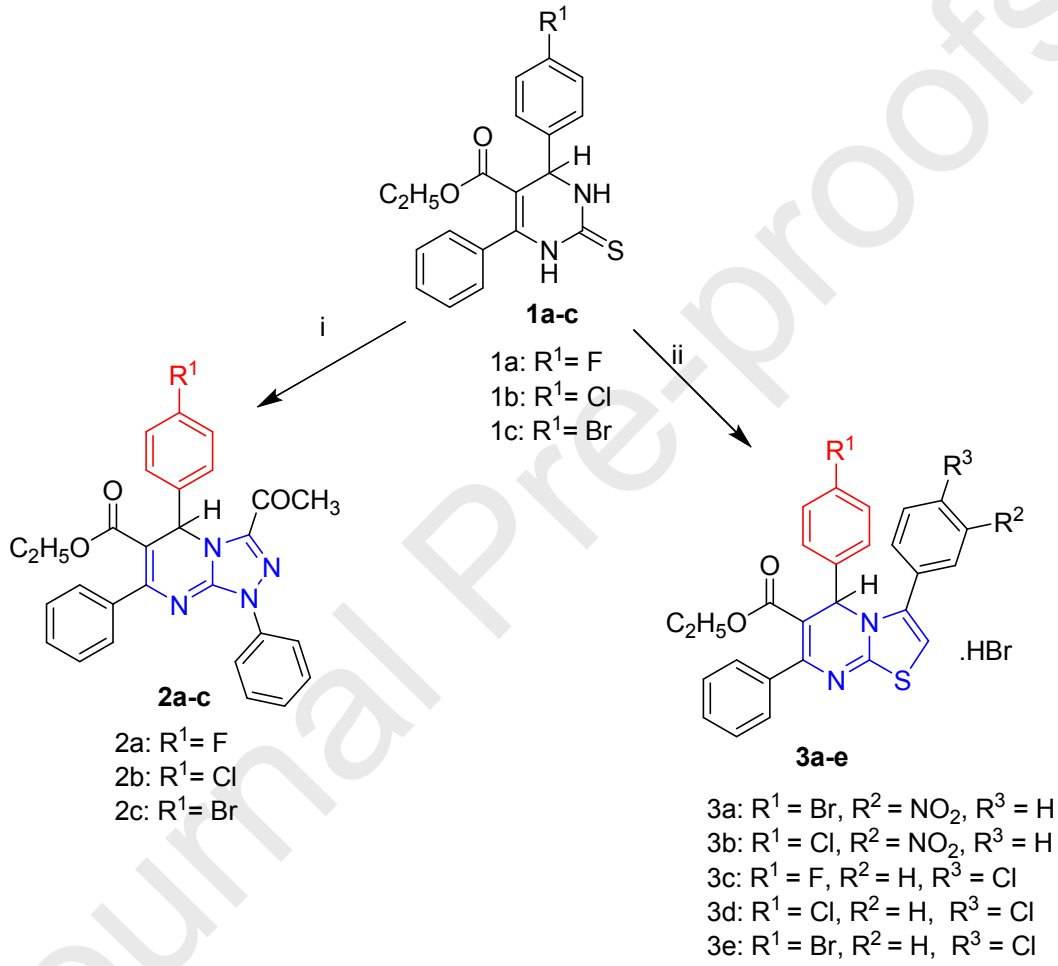

Synthesis of hydrazonoyl chloride derivative 4:

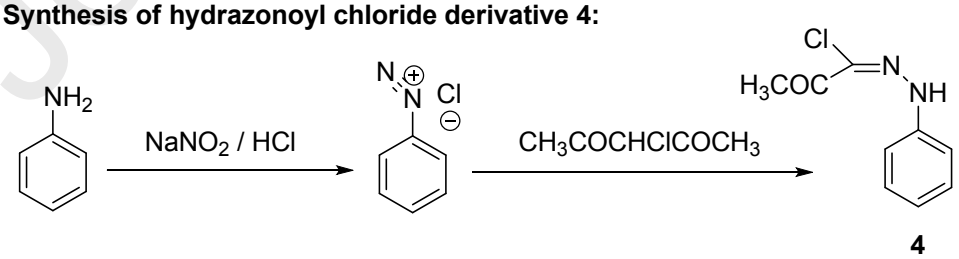

Scheme 1. Reagents: (i) **4** / TEA / Dioxane ii) 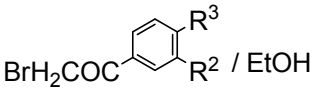 / EtOH

2. 2. Biological evaluation

2. 2. 1. *In vitro* anticancer screening

In vitro anticancer screening of the targeted compounds (**2a-c**, **3a-c**) was carried out by the National Cancer Institute (NCI), Bethesda, USA against 60 human cancer cell lines representing the following cancer types: leukemia, non-small cell lung, colon, CNS, melanoma, ovarian, renal, prostate, and breast cancers. Single dose screening assay (10^{-5}M concentration) was carried out with 48 h incubation of the cell. End point determination was carried out using sulforhodamine-B (SRB). Results were reported as a graph representing growth percent. The percent inhibition results were represented in **(Table *S1 in supplementary material*)**. Unfortunately, most of the synthesized compounds showed poor anticancer activity. However, compound **3d** exhibited selective significant cell growth inhibition above 90% against renal cell line (A 498). Compound **3d** also showed remarkable inhibitory effect against both leukemia cell line (K-562) and prostate cancer cell line (PC-3) with 68.54 and 58.73 growth inhibition percentage, respectively. Furthermore, its analogue **3a** bearing nitro and bromo substituents on the aromatic rings displayed good cell growth inhibition against melanoma (SK-MEL-5) and prostate cancer (PC-3) cell lines with 76.56 and 64.94, respectively. For the derivative **3e,** it was found that it showed moderate inhibitory cell growth inhibition against prostate cancer (PC-3) cell line. Neither the triazolopyrimidines (**2a-c**) nor the thiazolopyrimidine (**3b, 3c**) showed any significant cell growth inhibition under the same conditions.

2.2.2. *In vitro* cytotoxicity IC_{50} determination

Compound **3d** was further evaluated by determining the IC_{50} against A-498 renal cell line (most sensitive cell line) by the MTT colorimetric assay using doxorubicin as standard [25]. The results revealed that compound **3d** which demonstrated the most potent cytotoxic activity against renal cell line A-498 showed good inhibitory activity (with IC_{50} of 3.50 μM) compared to doxorubicin against A-498 renal cell line (with IC_{50} of 1.21 μM) (**Table 1**, **Fig. S2 in supplementary data**).

Table 1 Cytotoxic activity of compound **3d and** doxorubicin against renal cell line A-498.

Compound	3d(IC_{50}%)±S.D.*	Doxorubicin(IC_{50}%)±S.D.*
A-498	3.50 ± 0.20	1.21 ± 0.80

* S.D.: standard deviation

2.2.3. Cell cycle analysis

Cell cycle is a cascade of events that takes place in a cell and it is necessary for its division and replication. G1 phase, S phase (synthesis), G2 phase (collectively known as interphase) and M phase (mitosis) represented the four main distinct phases of the cell cycle. The G1-phase, also called post-mitotic pre-synthesis phase, characterized by following directly cell division. The S- phase is identified by DNA replication. The time when the cell prepares to split off in two cells, distinguished the G2-, premitotic or post-synthetic phase that can be considered the actual division. Finally, in the M- or mitosis-phase division, the doubled DNA organized in chromosomes is separated [26]. Flow cytometry analysis of the selected compound **3d** which showed the most cytotoxic activity against renal cell line A-498. Exposure of renal cell line A-498 to compound 3d at its IC_{50} concentration (3.50 μM) for 24 h and 48 h was shown to induce a remarkable disruption in cell cycle profile and cell-cycle arrest **(Fig. 2)**. Results showed that there was an increase in the percentage of apoptotic cells at the pre-G phase of 27.55% when treated with **3d** and 22.15% for doxorubicin when compared to control (1.79%). Reduction in the percentage of cells at G0/G1 and S phases to 26.67% and 24.77%, respectively compared to control A-498 renal cell line which showed 53.64% and 36.41%, respectively. Treating the same cells with doxorubicin resulted in a comparable reduction in G0-G1 and S cells (41.59% and 26.38%). On the other hand, increased population of cells at the G2/M phase when treated with compound **3d** to (48.54%) than control (9.95%) and more than that of doxorubicin (32.03%). Hence, it can be concluded that compound **3d** showed cell cycle arrest at G2/M phase which in turns leads to inhibition of cell proliferation and induced apoptosis (**Table 2**, **Fig. S3 supplementary material**)

Table 2 Effect of compound **3d,** doxorubicin and control on DNA-ploidy flow cytometric analysis of renal A-498 cells.

Cell cycle phase	%G0-G1	%S	%G2-M	%Pre G1
3d	26.67	24.77	48.54	27.55
Doxorubicin	41.59	26.38	32.03	22.15
Control	53.64	36.41	9.95	1.79

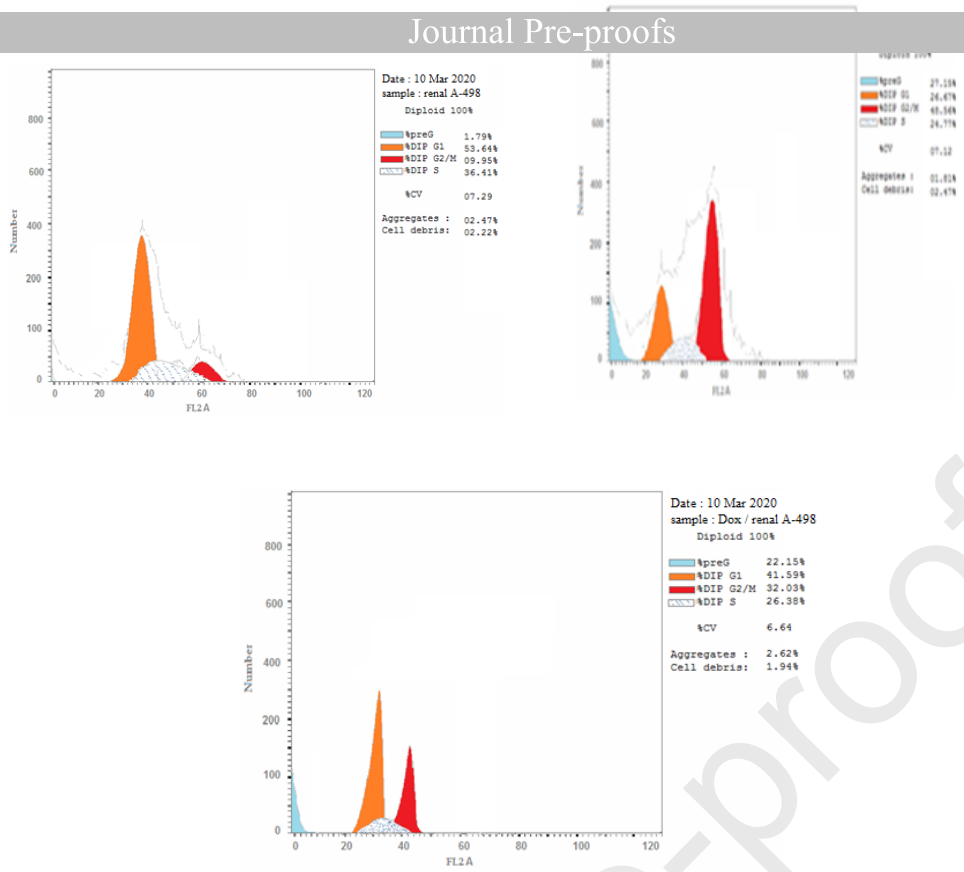

Fig. 2. Compound **3d** effect on DNA-ploidy flow cytometric analysis of renal A-498 cells compared to doxorubicin and negative control. Renal A-498 cells were treated with DMSO 0.01% or compound 3d at its (IC_{50} = 3.5 µM), for 24 h and 48 h, and the harvested cells were subjected to Cell-cycle analysis using a FACS Calibur flow cytometer.

2.2.4. Annexin-V apoptosis assay

To assure the apoptotic activity of compound **3d**, annexin-V apoptosis assay was performed on A-498 renal cancer cell line. This assay determines phosphatidylserine (PS) expressed on the surface of the apoptotic cells and fluoresces green upon interacting with the labelled Annexin V. The assay relies on that during apoptosis, membrane asymmetry is lost, and PS transfers from the cytoplasmic side of the membrane to the external leaflet. In this assay, propidium iodide (PI) is used which can cross only compromised membranes to intercalate DNA strands. Accordingly, PI can be used to determine the late stages of apoptosis by the presence of red fluorescence. The results showed an increase in annexin-V positive apoptotic cells at the early and late apoptotic stages to 8.34% (8.2 fold) and 15.82% (33.6 fold) respectively, while for doxorubicin 5.48% (4.6fold) and 14.2% (30.2fold) increase in early and late apoptosis respectively compared to control (1.2% and 0.47% respectively) (**Table 3**). Moreover, the percentage of necrosis caused by compound **3d** and doxorubicin was 2.99% and 2.47%, respectively which were significantly higher than control that showed only 0.3% necrosis **(Fig. 3**, **Fig. S4 in supplementary data)**.

Table 3 Effect of compound **3d,** doxorubicin and control treatment on induction of apoptosis.

Compounds	Total apoptosis	Early apoptosis	Late apoptosis	Necrosis
3d	27.15	8.34	15.82	2.99
Doxorubicin	22.15	5.48	14.2	2.47
Control	1.79	1.02	0.47	0.3

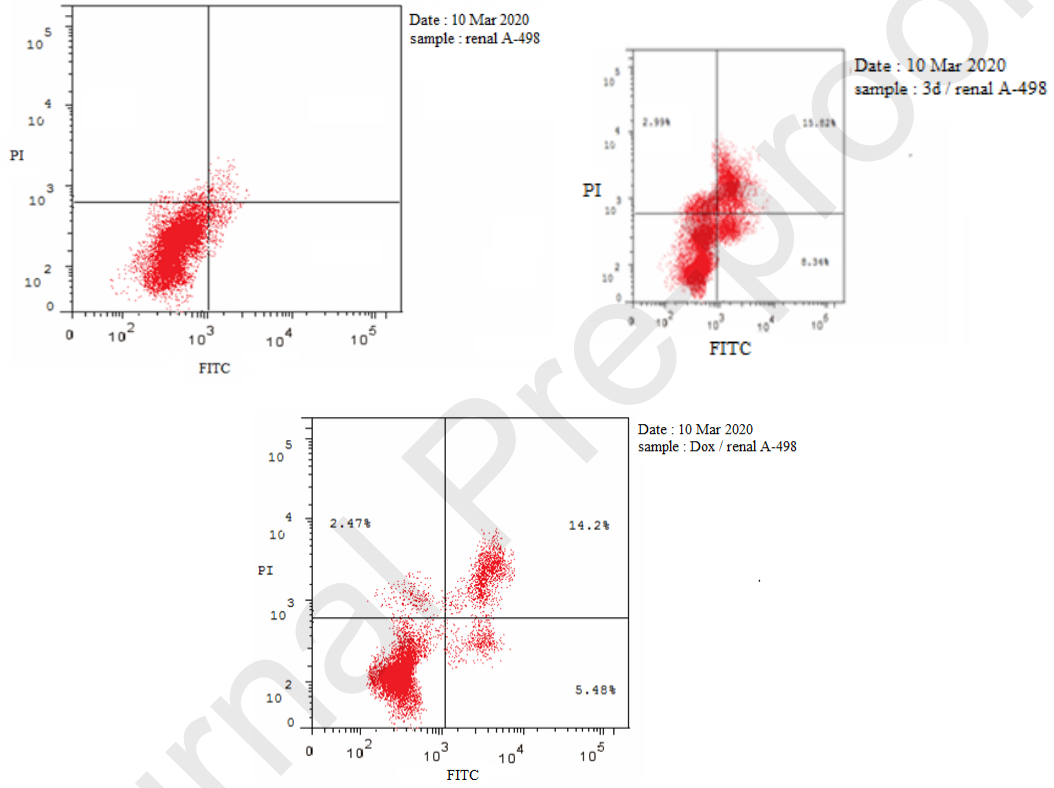

Fig. 3. Effect of compound **3d** treatment on induction of apoptosis. MCF-7 cells were treated with DMSO 0.01% or compound **3d** at its (IC_{50} = 3.5 µM) for 24 or 48h, the harvested cells were stained with Annexin V-FITC apoptosis detection kit and Analyzed on a Flow cytometer.

2.2.5. Topoisomerase II inhibitory activity

Regulation of the topological state of DNA strands is controlled by topoisomerases which are nuclear enzymes rule breaking and rejoining of DNA strands. The mechanism of action of topo II was reported to cause a transient enzyme bridged to DNA strands, as well as double-strand break, followed by strand passing and resealing thus affecting DNA

metabolism, replication and transcription [27]. In order to be more specific about the mechanism of action regarding the cytotoxic activity of compound **3d**. Searching the literature revealed that topoisomerase II is over expressed in A-498 cells [28-30]. For this reason, compound **3d** was evaluated for its inhibitory effect against topoisomerase II. Topoisomerase II inhibition percent were evaluated at five different concentrations (0.01, 0.1, 1, 10 and 100 mM) to calculate their IC_{50} values. Biological results revealed that compound **3d** showed potent inhibitory activity against topoisomerase IIα with IC_{50} of 2.89 μM compared to doxorubicin (IC_{50} = 2.67 μM) (**Table 4**). It is assumed that the inhibitory activity of compound **3d** may be attributed to its *S* isomer based on docking study prediction which was carried out.

Table 4 The topoisomerase II inhibition per cent of compound **3d, and** doxorubicin.

Compound	3d(IC_{50}%)±S.D.*	Doxorubicin(IC_{50}%)±S.D.*
Topoisomerase IIα	2.89 ± 0.72	2.67 ± 0.58

* S.D.: standard deviation

2.2.6. Molecular modeling study

Topoisomerase II alpha structure was obtained from protein data bank (PDB ID:5GWK) database [31]. Validation of molecular docking study was performed via docking of etoposide **I** in the DNA binding site which was able to bind in the active site of the enzyme with binding energy score -6.645 kcal/mol. (*S*) isomer of thiazolopyrimidine derivative **3d** was recognized in various interactions within the active site residues of topoisomerase II as displayed in (**Fig. 4**). From the docking results, it was noted that, **3d**-topoisomerase II complex possess good docking interaction energy of -5.436 kcal/mol. The predicted binding pattern of **3d** showed that the planar thiazole moiety embedded into the major groove of DNA. Both phenyl and thiazole rings forms π-π static interactions with guanine monophosphate (DG13). Moreover, compound **3d** also formed van der Waal's interaction with Gly 488 amino acid residue. It is worth mentioning that (*R*) isomer of the thiazolopyrimidine **3d** haven't been recognized to bind to the active site of topoisomerase II enzyme which revealed that *S* isomer is the active enantiomer that may be responsible for topoisomerase II inhibitory activity. Regarding the possibility of instability of compound **3d** metabolite due to the presence of acetylester group that could be easily degraded inside the body. Accordingly, the acid metabolite was subjected to redocking to find out its inhibitory effect. The acid metabolite was found to bind via two hydrogen bond donor interactions with Asp 463 and Arg 487 amino acid residues with binding energy score -5.270 kcal/mol comparable to its parent analogue (**Fig. 5**).

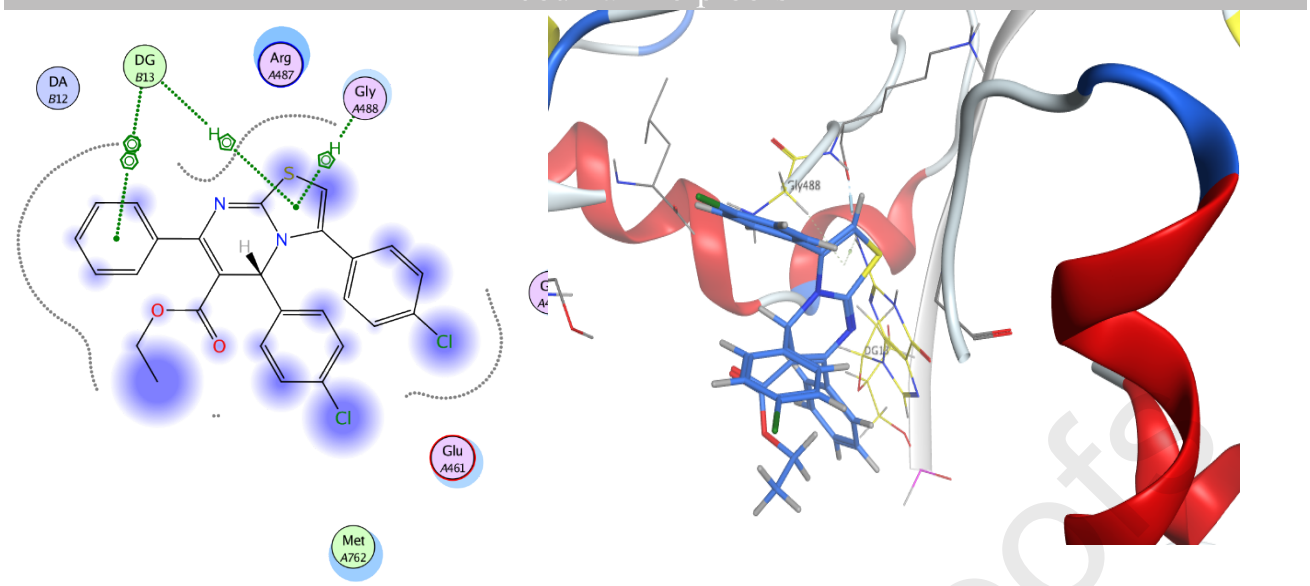

Fig. 4. (A) 2D caption of *S* isomer of compound **3d** in the binding site of topoisomerase II. (B) 3D caption of *S* isomer of compound **3d** colored with blue and active site of topoisomerase II colored with yellow.

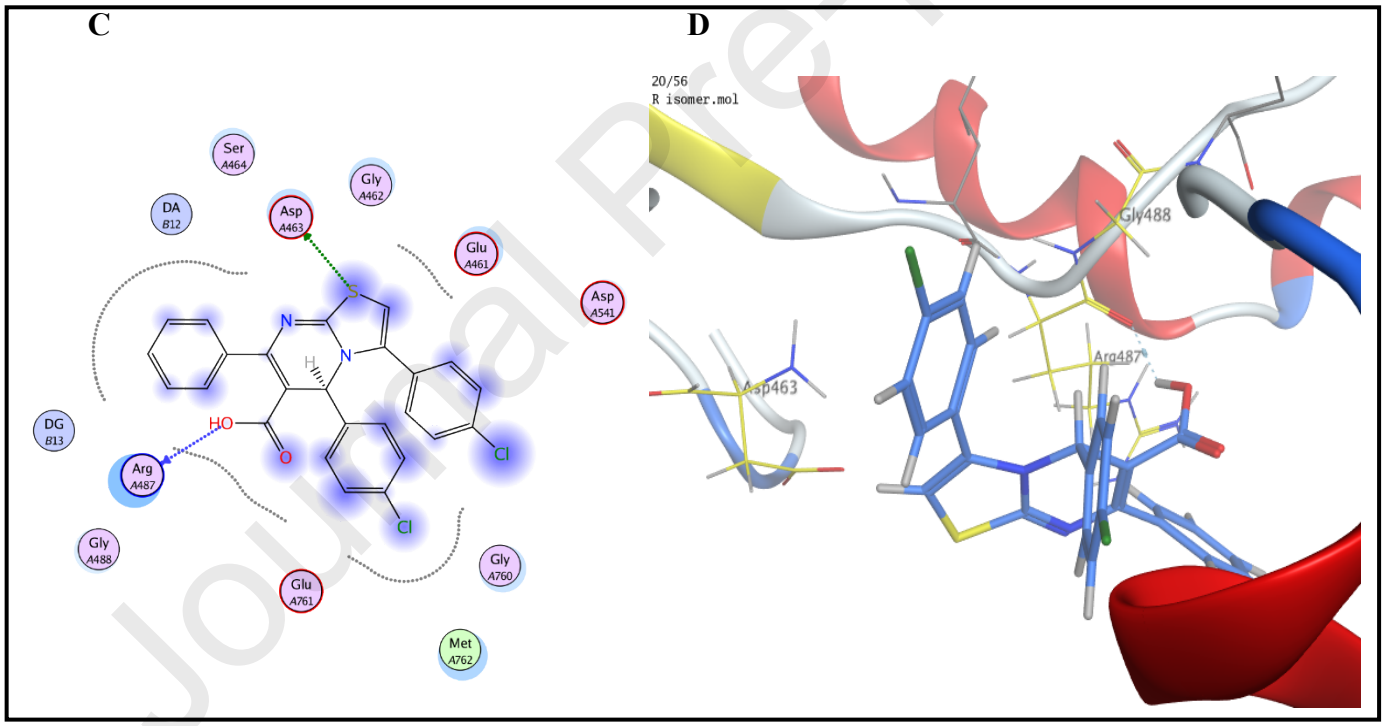

Fig. 5. (C) 2D caption of acid metabolite of compound **3d** in the binding site of topoisomerase II. (D) 3D interaction of acid metabolite of compound **3d** colored with blue binding to topoisomerase II (5GWK).

3. Conclusion

A series of triazolopyrimidines and thiazolopyrimidine hydrobromides were prepared and investigated for anticancer activity against 60 human cancer cell lines. Compound **3d**

revealed significant inhibition effect on renal cell line A498 with 92.46 % inhibition (IC_{50} 3.5 μM). Applying MTT colorimetric assay showed that compound **3d** exhibited a good inhibitory activity (IC_{50}=3.50 μM) compared to doxorubicin against A-498 renal cell line (IC_{50} = 1.21 μM). Moreover, cell cycle analysis showed cell cycle arrest of compound **3d** at G2/M phase leading to cell proliferation inhibition and pro-apoptotic activity. Performing the enzymatic assay of thiazolopyrimidine **3d** against topoisomerase II showed its potent inhibitory activity (IC_{50} =2.89 μM) compared with doxorubicin as reference compounds with (IC_{50} = 2.67 μM). Finally, the obtained results were confirmed with molecular modeling study of the synthesized compounds which demonstrate the ability of compound **3d** to embed in the groove of DNA as well as its binding to topoisomerase II enzyme binding site.

4. Experimental

4.1. Chemistry

Melting points are uncorrected and were determined on a Stuart melting point apparatus (Stuart Scientific, Redhill, UK). The IR spectra (KBr) were measured on Shimadzu IR 435 spectrophotometer and values are represented in cm^{-1}. ^{1}H NMR (300 MHz) and ^{13}C NMR (75 MHz) spectra were carried out using a Varian Gemini 300-BB spectrophotometer. (Bruker, Munich, Germany), using tetramethylsilane TMS as an internal standard. Splitting patterns were designated as follows: s: singlet; d: doublet; t: triplet; m: multiplet and Chemical shift values are recorded in ppm on δ scale. Progress of the reactions was monitored by TLC using TLC sheets precoated with UV florescent silica gel Merck 60 F 254 and was visualized using UV lamp. Chemicals used are supplied from Across (New Jersey, USA). Elemental analyses were performed at the Microanalytical Center, Al-Azhar University.

General procedure for the synthesis of compounds (**1a-c**): [32-35]

A ternary mixture of each of ethyl benzoylacetate (19.2g, 0.1mol), thiourea (7.6g, 0.1mol) and the appropriate aromatic aldehyde (0.1mol) in absolute ethanol (30ml) containing a catalytic amount of concentrated hydrochloric acid (10drops) was refluxed for 3 hours. The reaction mixture was then cooled to 0°C, the separated solid was collected by filteration, washed with ethanol and crystallized from ethanol to afford compounds **1a-c** as white solids: Yields 65-81%; m.p. (**1a**) 190-2 °C, (**1b**) 178-80 °C, (**1c**) 170-2 °C.

*Preparation of 2-Oxo-N-phenylpropanehydrazonyl chloride **4:*** [36]

To a stirred solution of 3-chloro-2,4-pentanedione (1.34g, 10 mmol) in 20 ml ethanol, sodium acetate trihydrate (5 gm) was added. After stirring for 15 minutes, the mixture was chilled at 0°C and treated with a cold solution of aniline (0.93g, 10 mmol) in hydrochloric acid (36%, 10ml) with sodium nitrite solution ((10 mmol of sodium nitrite in least amount

of water)). The addition of diazonium salt was carried out with rapid stirring over period of 30 minutes. The reaction mixture was stirred for additional 2 hours at 0-5 °C then left for 8 hours in a refrigerator. The resulting solid was collected by filtration and crystallized from ethanol: Yield, 80%; m.p. 160-2 °C.

General procedure for the synthesis of compounds **2a-c**:

A mixture of 2-thioxo derivative 1a-c (10 mmol), the appropriate hydrazonoyl chloride (10 mmol) was stirred under reflux in dioxane (30 ml) with 4 drops of triethylamine for 5 hours. The solvent was evaporated under reduced pressure. The solid produced was washed three times by 30 ml methanol, and crystallized from benzene to produce the compounds 2a-c.

Ethyl 3-acetyl-5-(4-fluorophenyl)-1,5-dihydro-1,7-diphenyl-[1,2,4] triazolo[4,3-a]pyrimidine-6-carboxylate **2a**:

Yellow solid: yield, 70%; m.p. 150-2 °C; IR (KBr) ν_{max}: 3109 (CH arom.), 2981, 2935 (CH aliph.), 1693-1680 (2C=O) cm^{-1}, ^1H NMR ($CDCl_3$) δ: 0.84 (t, *J* = 7.1 Hz, 3H, CH_3), 2.61 (s, 3H, CH_3), 3.88 (q, *J* = 7.1 Hz, 2H, CH_2), 5.55 (s, 1H), 7.01 (s, 1H, Ar-H), 7.07-7.11 (m, 2H, Ar-H), 7.36-7.39 (m, 3H, Ar-H), 7.43-7.50 (m, 4H, Ar-H), 7.61 (d, 2H, *J* = 8.2 Hz, Ar-H), 8.23 (d, 2H, *J* = 8.2 Hz, Ar-H) ppm. ^{13}C NMR (DMSO-d_6) δ: 13.6, 26.5, 55.9, 57.7, 59.8, 60.4, 103.7, 116.0, 120.6, 127.4 (d), 128.2 (d), 128.6, 128.7 (d), 129.2 (d), 133.9, 137.0, 141.0, 143.7, 148.8, 157.5, 166.3, 187.4 ppm. Anal. Calcd. For $C_{28}H_{23}FN_4O_3$: C, 69.70; H, 4.80; N, 11.61. Found: C, 69.12; H, 4.70; N, 11.38 %.

Ethyl 3-acetyl-5-(4-chlorophenyl)-1,5-dihydro-1,7-diphenyl-[1,2,4] triazolo[4,3-a]pyrimidine-6-carboxylate **2b**:

Yellow solid: yield, 76%; m.p. 170-2 °C; IR (KBr) ν_{max}: 3059 (CH arom.), 2978, 2939 (CH aliph.), 1701, 1681 (2C=O) cm^{-1}, ^1H NMR (DMSO-d_6) δ: 1.41 (t, *J* = 6.9 Hz, 3H, CH_3), 2.58 (s, 3H, CH_3), 3.70 (s, 1H), 3.90 (q, *J* = 6.9 Hz, 2H, CH_2), 6.97 (s, 1H, Ar-H), 7.37 (m, 5H, Ar-H), 7.45-7.48 (m, 4H, Ar-H), 7.52 (d, 2H, *J* = 8.2 Hz, Ar-H), 8.20 (d, 2H, *J* = 8.2 Hz, Ar-H) ppm. ^{13}C NMR (DMSO-d_6) δ: 8.7, 13.6, 26.5, 45.9, 57.7, 59.8, 67.0, 100.4, 120.6, 127.5, 128.6, 128.8, 128.8, 129.2, 134.4, 136.9, 140.9, 141.4, 148.7, 157.3, 166.2, 187.3 ppm. Anal. Calcd. For $C_{28}H_{23}ClN_4O_3$: C, 67.40; H, 4.65; N, 11.23. Found: C, 66.97; H, 5.11; N, 11.26 %.

Ethyl 3-acetyl-5-(4-bromophenyl)-1,5-dihydro-1,7-diphenyl-[1,2,4] triazolo[4,3-a]pyrimidine-6-carboxylate **2c**:

Yellow solid: yield, 74%; m.p. 175-7 °C; IR (KBr) ν_{max}: 3062, 3028 (CH arom.), 2978 (CH aliph.), 1701, 1678 (2C=O) cm^{-1}, ^1H NMR (DMSO-d_6) δ: 0.89 (t, *J* = 7.1 Hz, 3H, CH_3), 2.60 (s, 3H, CH_3), 3.72 (s, 1H), 3.89 (q, *J* = 7.1 Hz, 2H, CH_2), 6.98 (s, 1H, Ar-H), 7.36-7.39 (m, 5H, Ar-H), 7.44-7.46 (m, 4H, Ar-H), 7.49 (d, 2H, *J* = 8.2 Hz, Ar-H), 8.24

(d, 2H, *J* = 8.2 Hz, Ar-H) ppm. ^{13}C NMR (DMSO-d_6) δ: 13.6, 26.5, 57.9, 59.8, 67.1, 100.4, 157.5, 166.2, 187.3 ppm. Anal. Calcd. For $C_{28}H_{23}BrN_4O_3$: C, 61.89; H, 4.27; N, 10.31. Found: C, 61.76; H, 4.28; N, 9.81 %.

General procedure for the synthesis of compounds (**3a-e**):

A solution of each of **1a-c** (0.01mol) and appropriate substituted phenacyl bromide (0.01mol) in absolute ethanol (50ml) was heated under reflux for 10 hours. The precipitate formed on standing at room temperature was collected by filteration and crystallized from ethanol to afford compounds **3a-e**.

Ethyl 5-(4-bromorophenyl)-3-(3-nitrophenyl)-7-phenyl-5H-thiazolo[3,2-a] pyrimidine-6-carboxylate hydrobromide **3a**:

Yellow solid: yield, 74%; m.p. 196 °C; IR (KBr) ν_{max}: 3086 (CH arom.), 2931 (CH aliph.), 1708 (C=O) cm^{-1}, ^{1}H NMR (DMSO-d_6) δ: 0.78 (t, *J* = 6.8 Hz, 3H, CH_3), 3.80 (q, *J* = 6.8 Hz, 2H, CH_2), 5.89 (s, 1H, C_5-H), 6.74 (d, *J* = 5.9 Hz, 2H, Ar-H), 7.11 (d, *J* = 6.8 Hz, 2H, Ar-H), 7.42-7.50 (m, 5H, Ar-H), 7.51 (d, *J* = 5.9 Hz, 2H, Ar-H), 7.60 (s, 1H, Ar-H), 8.04 (d, *J* = 6.8 Hz, 2H, Ar-H), 12.35 (s, 1H) ppm. ^{13}C NMR (DMSO-d_6) δ: 13.5, 58.0, 61.0, 89.1, 97.3, 102.3, 109.5, 115.1, 123.8, 125.5, 126.2, 128.5, 129.3, 130.5, 130.8, 131.9, 132.1, 135.7, 138.5, 140.7, 147.8, 156.5, 166.5 ppm. Anal. Calcd. For $C_{27}H_{20}BrN_3O_4S$.HBr: C, 50.41; H, 3.29; N, 6.53. Found: C, 49.64; H, 3.65; N, 6.46 %.

Ethyl 5-(4-chlorophenyl)-3-(3-nitrophenyl)-7-phenyl-5H-thiazolo[3,2-a] pyrimidine-6-carboxylate hydrobromide **3b**:

Yellow solid: yield, 76%; m.p. 185-187 °C ; IR (KBr) ν_{max}: 3105, 3043 (CH arom.), 2981 (CH aliph.), 1693 (C=O) cm^{-1}, ^{1}H NMR (DMSO-d_6) δ: 0.79 (t, *J* = 7.2 Hz, 3H, CH_3), 3.86 (q, *J* = 7.2 Hz, 2H, CH_2), 6.36 (s, 1H, C_5-H), 6.81 (d, *J* = 8.4 Hz, 2H, Ar-H), 6.95 (d, *J* = 8.3 Hz, 1H, Ar-H), 7.21 (d, *J* = 8.4 Hz, 2H, Ar-H), 7.36-7.57 (m, 5H, Ar-H), 7.64-7.72 (m, 2H, Ar-H), 8.00 (s, 1H, Ar-H), 8.42 (d, *J* = 8.3 Hz, 1H, Ar-H), 13.19 (s, 1H) ppm. ^{13}C NMR (DMSO-d_6) δ: 13.3, 59.6, 61.2, 96.9, 103.4, 116.6, 124.8, 125.6, 128.0, 128.3, 129.1, 129.5, 130.4, 130.8, 131.5, 135.9, 136.0, 136.5, 137.0, 143.2, 148.0, 160.9, 164.1 ppm. Anal. Calcd. For $C_{27}H_{20}ClN_3O_4S$.HBr: C, 54.15; H, 3.53; N, 7.02. Found: C, 54.37; H, 3.70; N, 7.31%.

Ethyl 3-(4-chlorophenyl)-5-(4-fluorophenyl)-7-phenyl-5H-thiazolo[3,2-a] pyrimidine-6-carboxylate hydrobromide **3c**:

Yellow solid: yield, 74%; m.p. 226-228 °C; IR (KBr) ν_{max}: 3113, 3047 (CH arom.), 2978 (CH aliph.), 1697 (C=O) cm^{-1}, ^{1}H NMR (DMSO-d_6) δ: 0.70 (t, *J* = 7.2 Hz, 3H, CH_3), 3.77 (q, *J* = 7.2 Hz, 2H, CH_2), 6.44 (s, 1H, C_5-H), 6.87-6.91 (m, 2H, Ar-H), 7.04-7.08 (m, 2H,

Ar-H), 7.40 (d, *J* = 8.4 Hz, 2H, Ar-H), 7.50-7.54 (m, 6H, Ar-H), 7.61 (d, *J* = 8.4 Hz, 2H, Ar-H) ppm. ^{13}C NMR (DMSO-d_6) δ: 13.3, 59.2, 61.1, 103.1, 115.2, 115.4, 116.1, 116.3, 128.0, 128.7, 129.0, 129.4, 129.6, 129.7, 130.6, 132.0, 136.1, 139.0, 161.3, 161.4, 163.7, 164.2 ppm. Anal. Calcd. For $C_{27}H_{20}ClFN_2O_2S.HBr$: C, 56.70; H, 3.70; N, 4.90. Found: C, 57.10; H, 4.06; N, 4.92 %.

Ethyl 3-(4-chlorophenyl)-5-(4-chlorophenyl)-7-phenyl-5H-thiazolo[3,2-a] pyrimidine-6-carboxylate hydrobromide **3d**:

Yellow solid: yield, 80%; m.p. 220-2 °C; IR (KBr) ν_{max}: 3001 (CH arom.), 2873 (CH aliph.), 1693 (C=O) cm^{-1}, ^{1}H NMR (DMSO-d_6) δ: 0.80 (t, *J* = 7.2 Hz, 3H, CH_3), 3.87 (q, *J* = 7.2 Hz, 2H, CH_2), 6.38 (s, 1H, C_5-H), 6.81 (d, *J* = 8.4 Hz, 2H, Ar-H), 7.14 (d, *J* = 8.0 Hz, 2H, Ar-H), 7.21 (d, *J* = 8.4 Hz, 2H, Ar-H), 7.32 (s, 1H, Ar-H),7.42-7.47 (m, 5H, Ar-H), 7.54 (d, *J* = 8.0 Hz, 2H, Ar-H), 13.4 (s, 1H) ppm. ^{13}C NMR (DMSO-d_6) δ: 13.3, 59.1, 61.1, 103.1, 115.3, 125.2, 128.0, 128.2, 129.2, 129.3, 129.3, 130.7, 131.1, 131.6, 135.6, 137.3, 137.3, 137.8, 143.7, 160.7, 164.3 ppm. Anal. Calcd. For $C_{27}H_{20}Cl_2N_2O_2S.HBr$: C, 55.12; H, 3.60; N, 4.76. Found: C, 54.97; H, 3.30; N, 4.65%.

Ethyl 5-(4-bromophenyl)-3-(4-chlorophenyl)-7-phenyl-5H-thiazolo[3,2-a] pyrimidine-6-carboxylate hydrobromide **3e**:

Yellow solid: yield, 80%; m.p. 232-4 °C; IR (KBr) ν_{max}: 3039, 3001 (CH arom.), 2874 (CH aliph.), 1693 (C=O) cm^{-1}, ^{1}H NMR (DMSO-d_6) δ: 0.79 (t, *J* = 7.2 Hz, 3H, CH_3), 3.86 (q, *J* = 7.2 Hz, 2H, CH_2), 6.37 (s, 1H, C_5-H), 6.74 (d, *J* = 8.4 Hz, 2H, Ar-H), 7.14 (d, *J* = 8.0 Hz, 2H, Ar-H), 7.34 (s, 1H, Ar-H), 7.36 (d, *J* = 8.4 Hz, 2H, Ar-H), 7.39-7.46 (m, 5H, Ar-H), 7.53 (d, *J* = 8.0 Hz, 2H, Ar-H), 13.31 (s, 1H) ppm. ^{13}C NMR (DMSO-d_6) δ: 13.3, 59.2, 61.1, 103.1, 115.2, 123.9, 125.2, 128.3, 129.1, 129.4, 130.8, 131.1, 131.6, 132.0, 132.3, 137.4, 137.8, 137.9, 143.7, 160.7, 164.3 ppm. Anal. Calcd. For $C_{27}H_{20}BrClN_2O_2S.HBr$: C, 51.25; H, 3.34; N, 4.43. Found: C, 50.63; H, 3.19; N, 4.30%.

4.2. Biological evaluation

4.2.1. *In vitro* antitumor screening

Antitumor screening of the synthesized compounds was carried out as reported standard procedure [37-39] where the human tumor cell lines were grown in RPMI 1640 medium containing 2mM L-glutamine and 5% fetal bovine under sterile conditions. Cells were inoculated into 96 well microtiter plates into 100 μL at an optical density ranging from 5000 to 40,000 cells/well depending on the doubling time of individual cell lines. Each

compound was dissolved in dimethyl sulfoxide (DMSO), So each final dilution has less than 1% DMSO. The prepared compounds (100 µL) were pipetted into the appropriate well of a microtiter tray in duplicate. The cultures were incubated at 37 °C in a humidified incubator. In addition, the incubator was supplied with 5% CO2 atmosphere. After 48 h, Trichloroacetic acid was added to fix the cells 50 µL of cold 50% (w/v) and the plates were incubated for 60 min at 4 °C. The supernatant was discarded and the plates are washed 5 times with tap water and air dried. Sulphorhodamine B (SRB) solution (100 µL) at 0.4% (w/v) in 1% acetic acid was added to each well then plates incubation occur for 10 min at room temperature. Unbound dye was removed by washing 5 times with acetic acid (1%) and plates were air dried. The bound dye was solubilized in 10 µM trizma base and the absorbance was read at 515 nm wavelength using an automated plate reader. The treated cells percentage growth was calculated in a ratio to the untreated control cells.

4.2.2. MTT assay for viability of cell

MTT colorimetric assay was used to determine the IC_{50} against A-498 renal cell line (most sensitive cell line) by the using doxorubicin as standard [40]. Where renal A-498 cells were grown in 100 µL Dulbecco's Modified Eagle's Medium **DMEM** media in 96-well cell culture plate, supplemented with 1% penicillin / streptomycin and were incubated at 37 °C till the concentration of the cells in the media was 5×104 cells/mL.

Cells were inoculated into 96 well microtiter plates into 100 µL at an optical density ranging from 4000 to 5000 cells/well depending on the replication time of individual cell lines. The tested compound and standards were solubilized in DMEM media at 1 mg/mL concentration. 10 fold serial dilutions to get the final concentrations (0.01-100 µM) and were incubated for 24 h. 50 µL/well of MTT (3-(4,5-dimethylthiazol-2-yl)-2,5-diphenyltetrazolium bromide was dissolved in in phosphate buffered saline and incubate the cultures at 37 °C for 4 h with 5% CO_2. 100 µL of isopropanol / 0.04 N HCl was added to all wells and mixed to dissolve the formed blue crystals. The absorbance was read on Robonik P2000 spectrophotometer at a wavelength of 490 nm.

4.2.3. Cell cycle analysis

DNA-flow cytometry analysis was carried out in order to study the effect of compound **3d** on cell cycle progression [41]. Where, renal A-498 cells were exposed to compound **3d** (IC_{50} = 3.5 µM) for 24 h. The cells were washed with ice-cold phosphate buffer saline (PBS), collected by centrifugation, fixed in 70% (v/v) ethanol, washed with PBS and re-suspended with 0.1 mg/mL RNase. Moreover, cells were stained with 40 mg/mL propidium iodide (PI) and cell cycle distribution was determined using FACSCalibur flow

cytometer (Becton Dickinson) and calculated using Cell Quest software (Becton Dickinson).

4.2.4. Annexin V-FITC apoptosis Determination

Apoptotic effect of compound **3d** was done using Annexin-V-FITC [41]. Renal A-498 cells were incubated for 24 h after exposure to compound **3d** at its IC_{50} = 3.5 μM. The cells were collected, washed twice with PBS and stained with mixture of fluorescein isothiocyanate (FITC), Annexin-V- and PI (propidium iodide) and left for 30 min at room temperature in the dark. Analysis was performed using FACSCalibur flow cytometer (BD Biosciences, San Jose, CA, USA)**.**

4.2.5. Topoisomerase II inhibitory activity

Topoisomerase IIα inhibitory activity of compound **3d** was determined using the human DNA topoisomerase Elisa kit (Abcam, Japan. Recombinant Human Topoisomerase II alpha protein (ab159735)). Where, compound **3d** or doxorubicin (100 μL) were added to the wells and incubated at 37 °C for 1 h then Biotin-conjugated antibody solution was added to each well followed by incubation for 1 h at 37 °C. Allow plates to aspirate. Avidin conjugated Horseradish Peroxidase (HRP-avidin) solution (100 μL) was added to the wells, incubated again for 1 h at 37 °C. Add TMB substrate to the wells and the plate was incubated for 30 min at 37 °C, protect from light. The absorbance was read using spectrophotometer at a wavelength of 450 nm**.**

4.2.6. Molecular modeling study

Molecular modeling study was carried out using Molecular Operating Environment (MOE, 2014.0901) software. All minimizations were carried out with MOE with MMFF94x force field and automatic calculation of the partial and formal charges was carried out. The crystal structures of topoisomerase IIα was obtained from the protein data bank (PDB ID: 5GWK) database [31]. Optimization of hydrogen bond interactions and removal of the co-crystallized ligand was carried out to prepare the enzyme for docking steps. 3D protonation of the topoisomerase IIα. The docking protocol used was triangle matcher placement method and London DG scoring function. In order to validate the docking steps, docking of the standard topoisomerase inhibitor etoposide and comparing the results with studies reported in literature were analyzed [42].

Compliance with ethical standards

Disclosure of potential conflicts of interest: Authors declare that they have no conflict of interest.

Research involving human participants and/ or animals: No human volunteers or animals were used in this work.

Funding: This work is self funded.

Ethics approval and consent to participate: Not applicable.

Acknowledgement: The authors express their appreciation and thanks to Dr Hossam M. Hassan, Associate Professor, Pharmacognosy Department, Nahda University (NUB), Beni-Suef, Egypt, for his kind support and help provided during this work.

References

1. Cancer facts and figures ACS 2019, https://www.cancer.org/content/dam/cancerorg/research/cancer-facts-and statistics/annual-cancer-facts-and-figures/2019/cancerfacts-and-figures-2019.pdf.
2. M. Mohammadian, R. Pakzad, F. Towhidi, B.R. Makhsosi, A. Ahmadi, H. Salehiniya, *Clujul Med*., 2017, **90**, 286-293.
3. N. Wambang , N. Schifano-Faux , A. Aillerie, B. Baldeyrou, C. Jacquet, C. Bal-Mahieu, T. Bousquet, S. Pellegrini, P. T. Ndifon, S. Meignan, J.F. Goossens , A. Lansiaux, L. Pélinski, *Bioorg. Med. Chem*., 2016, **24**, 651–660.
4. A. Montecucco, F. Zanetta, G. Biamonti1, *EXCLI Journal*, 2015, **14**, 95-108.
5. F. M. Farsani , M. R. Ganjalikhany , S. Vallian, *Curr Cancer Drug Targets*, 2017, **17**, 657-668.
6. S. Deng, T. Yan, C. Jendrny, A. Nemecek, M. Vincetic, U.Gödtel- Armbrust, L. Wojnowski, *BMC Cancer,* 2014, **14**, 842- 854.
7. J. Banothu, M. Khanapur, S. Basavoju, R. Bavantula, M. Narra, S. Abbagani*, RSC Adv.*, 2014, **4**, 22866-22874.
8. N. Y. M. Abdo, *Acta Chim. Slov.* 2015, **62**, 168–180.
9. G. S. Hassan, S. M. El-Messery, A. Abbas, *Bioorg. Chem.* 2017, **74**, 41–52.
10. M. M. Mohamed, A. K. Khalil, E. M. Abbass, A. M. El-Naggar, *Synth. Commun*., 2017, **47**, 1441-1457.
11. R. A. Ali, E. R. El-Bendary, M. A. Ghaly, I. A. Shehata, *Der Pharma Chemica*, 2018, **10**, 36-42
12. T. Sekhar, P. Thriveni, A. Venkateswarlu, T. Daveedu, K. Peddanna, S. Sainath, *Spectrochimica Acta Part A: Molecular and Biomolecular Spectroscopy,* 2020, **231**, 118056.
13. F. A. M. Al-Omary, G. S. Hassan, S. M. El-Messery, H. I. El-Subbagh, *Eur. J. Med. Chem.* 2012, **47**, 65-72.
14. L.Y. Ma, B. Wang, L.P. Pang, M. Z., S.Q. Wang, Y.C. Zheng, K.P. Shao, D.Q. Xue, H.M. Liu, *Bioorg. Med. Chem. Lett.,* 2015, **25** , 1124–1128.
15. H. Nagarajalah I. M. Khazib, N. S. Begum, *J. Chem. Sci.,* 2012, **124**, 847–855.

16. S. Kolb, O. Mondesert, M. L. Goddard, D. Jullien, B. O. Villoutreix, B. Bucchinani, C. Garbay, Z. Binetruy, *Chem. Med. Chem.*, 2009, **4**, 833–843.
17. P. A. Channara, A. Saeeda, F. A. Larika, S. Rashidb, Q. Iqbala , M. Rozib , S. Younisb , J. Mahar, *Biomedicine & Pharmacotherapy*, 2017, **94**, 499–513.
18. M. Yıldırım, D. Çelike, Mol Divers, 2015, **19**, 1–13.
19. S. G. Abdel Moty, M. A. Hussein, S. A. Abdel Aziz , M. A. Abou-Salim, *Saudi Pharmaceutical Journal*, 2016, **24**, 119-132.
20. Mahmoud N. M. Yousif, Wael A. El-Sayed, Hebat-Allah S. Abbas, Hanem M. Awad, Nabil M. Yousif, Journal of Applied Pharmaceutical Science, 2017, 7, 21-32.
21. P. Biginelli; *Gazz. Chim. Ital.*, 1893, **23**, 360-416.
22. H. M. Hassneen, T. A. Abdllah, *Molecules*, 2003, **8**, 333-341.
23. A. Balkan, S. Uma, M. Ertan, W. Wiegrebe, *Pharmazie*, 1992, **47**, 687-688.
24. A. Balkan, M. Ertan, T. Burgemeister, *Arch. Pharm. (Weinheim, Ger.),* 1992, **325**, 499-501.
25. S. M. Sherif, M. M. Youssef, K. M. Mobarak, A.-S. M Abdel- Fattah, *Tetrahedron*, 1993, **49**, 9561-9572.
26. S. Elmeligie, A. M. Aboul-Magd, D. S. Lasheen, T. M. Ibrahim, T. M. Abdelghany, S. M. Khojah , K. A. M. Abouzid, *J Enzyme Inhib Med Chem*, 2019, **34**, 1347–1367
27. H. K. Rhee, H. J. Park, S. K. Lee, C.O. Lee, H. Y. P. Choo, *Bioorg Med Chem*, 2007, **15**, 1651–1658
28. T. Mosmann, *J. Immunol. Methods,* 1983, **65**, 55-63.
29. S. Y. Wu, S.L. Pan, Z.Y. Xiao, J.L. Hsu, M.C. Chen, K.H. Lee, C.M. Teng, *PLOS ONE*, 2014, **9**, e112220.
30. W. T. Beck, S. E. Morgan, Y.Y. Mo, U. G. Bhat, *Drug Resist Update*, 1999, **2**, 382-389.
31. Y.R. Wang, S.F. Chen, C.C. Wu, Y.W. Liao, T.S. Lin, K.T. Liu, Y.S. Chen, T.K. Li, T.C. Chien, N.L. Chan, *Nucleic Acids Res*, 2017, **45**, 10861-10871
32. D. Bozsing, P. Sohar, G. Gigler, G. Kovacs, *Eur. J. Med. Chem.*1996, **31**, 663.
33. I. M. F. Magda, E. A. M. Nehad, R. S. Heba, E. Mohey, A. A. Yousry, *Arz. Forsch*. 2006, **56**, 322-327.
34. S. Ramalingam, K. Pradeep, *Synth. Commun*. 2009, **39**, 1299-1309.
35. P. Pathak; *J. Chem. Pharm. Res.,* 2014, **6**, 1207-1211.
36. R. N. Lacey, *J. Chem. Soc*. 1954, 839-844.

37. M.C. Alley, D.A. Scudiere, A. Monks, M.L. Hursey, M.J. Czerwinski, D.L. Fine, [illegible] 601.
38. M.R. Boyd, K.D. Paull, *Drug Dev. Res*. 1995, **34**, 91–109.
39. M.R. Grever, S.A. Schepartz, B.A. Chabner, *Semin. Oncol*. 1992, **19**, 622–638.
40. D.T. Vistica, P. Skehan, D. Scudiero, A. Monks, A. Pittman, M.R. Boyd, *Cancer Res*.1991,**51**, 2515–2520.
41. M.F. Tolba, A. Esmat, A.M. Al-Abd, S.S. Azab, A.E. Khalifa, H.A. Mosli, S.Z. Abdel-Rahman, A.B. Abdel-Naim, *Int. Union* Biochem. *Mol. Biol*. 2013, **65**, 716–729.
42. N. Tripathi,N. Shaikh, P. V. Bharatam, P. Garg, *Mol. Inf*. 2019, **38**, 1800046

New triazolopyrimidine and thiazolopyrimidine derivatives as topoisomerase II inhibitors: Their design, synthesis, apoptotic inducing activities and molecular docking studies

[1], Asmaa M. AboulMagd [2*] Mohamed T. M. Nemr

Highlights

1. New series of triazolopyrimidines and thiazolopyrimidine hydrobromides was designed and prepared as topoisomerase II inhibitors.
2. Compound **3d** was the most potent inhibitor especially against the renal cell line A498 with IC_{50} = 3.5 μM.
3. Thiazolopyrimidine **3d** showed potent topoisomerase II inhibitory activity (IC_{50} 2.89 μM).
4. Docking study was performed and binding interactions of compound **3d** in the binding site of topoisomerase II enzyme rationalizing the significant inhibitory activity of this derivative.

New triazolopyrimidine and thiazolopyrimidine derivatives with anticancer activity: synthesis, topoisomerase II inhibitor, apoptotic inducing activity and molecular modeling study

Mohamed T. M. Nemr [1], Asmaa M. AboulMagd [2*]

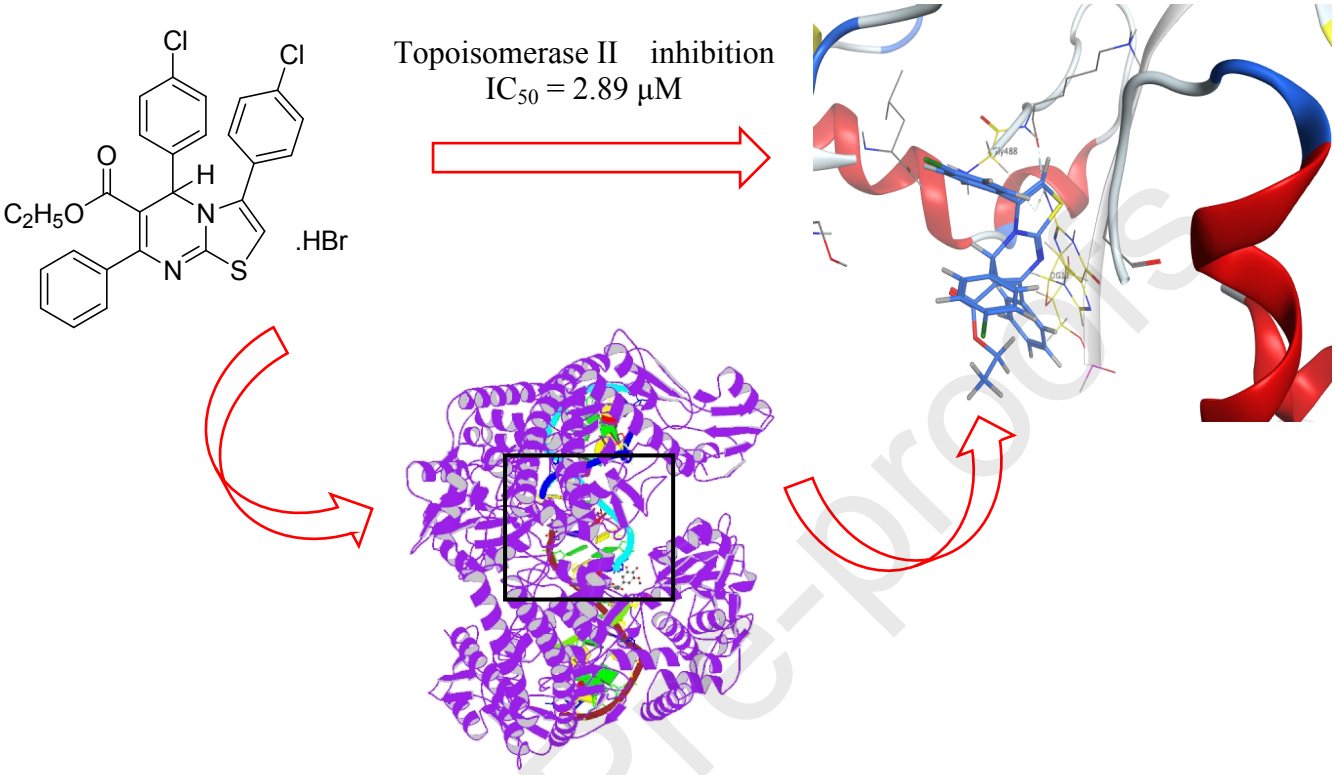

The thiazolopyrimidine hydrobromide derivative; **3d** showed 92.46 % inhibition on renal cancer cell line A498 with IC_{50} = 3.5 µM as well as cell cycle arrest at G2/M phase that indicated its apoptotic activity.